

# Chemical characteristics of chromian spinel in plutonic rocks: Implications for deep magma processes and discrimination of tectonic setting

著者	Arai Shoji, Okamura Hidenobu, Kadoshima Kazuyuki, Tanaka Chima, Suzuki Kenji, Ishimaru Satoko
journal or publication title	Island Arc
volume	20
number	1
page range	125-137
year	2011-03-01
URL	<a href="http://hdl.handle.net/2297/27101">http://hdl.handle.net/2297/27101</a>

doi: 10.1111/j.1440-1738.2010.00747.x



18 lower in plutonics than in volcanics at a given tectonic environment. The Cr# of spinels  
19 in plutonic rocks is highly diverse; its ranges overlap between the three settings, but  
20 extend to higher values (up to 0.8) in arc and oceanic hotspot environments. The Ti  
21 content of spinels in plutonics increases, for a given lithology, from the arc to oceanic  
22 hotspot settings via mid-ocean ridge on average. This chemical diversity is consistent  
23 with that of erupted magmas from the three settings. If we systematically know the  
24 chemistry of chromian spinels from a series of plutonic rocks, we can estimate their  
25 tectonic environments of formation. The spinel chemistry is especially useful in dunitic  
26 rocks, in which chromian spinel is the only discriminating mineral. Applying this,  
27 discordant dunites cutting mantle peridotites were possible precipitated from arc-related  
28 magmas in the Oman ophiolite, and from an intraplate tholeiite in the Lizard ophiolite,  
29 Cornwall.

30

31 **Key words:** ultramafic plutonics, chromian spinel, tectonic setting, Ti content, Cr/(Cr +  
32 Al) ratio

33 **Running title:** Chromian spinel in plutonic rocks

34

35

## 36 INTRODUCTION

37 Chromian spinel is common to ultramafic and related rocks, and is a very good indicator

38 of petrological characteristics of involved magmas (e.g. Irvine 1965, 1967; Dick &amp;

39 Bullen 1984; Roeder 1994; Kamenetsky *et al.* 2001). It has a general formula,  $(\text{Mg},$ 40  $\text{Fe}^{2+})(\text{Cr}, \text{Al}, \text{Fe}^{3+})_2\text{O}_4$ , where  $\text{Fe}^{3+}$  is only minor in peridotitic rocks.  $\text{Cr}/(\text{Cr} + \text{Al})$  atomic

41 ratio (= Cr#) is highly variable and serves as an important petrogenetic indicator for

42 ultramafic and related rocks (Irvine 1967; Dick & Bullen 1984).  $\text{Mg}/(\text{Mg} + \text{Fe}^{2+})$  atomic

43 ratio (= Mg#) varies inversely with the Cr# in chromian spinel (e.g. Irvine 1967). Small

44 amounts of Ti are possibly incorporated as  $\text{Fe}_2\text{TiO}_4$  (= ulvospinel component) in

45 chromian spinel. Arai (1992) summarized the chemistry of chromian spinel in volcanic

46 rocks (or magmas) as a potential indicator of magma chemistry for three main tectonic

47 settings, *i.e.*, the mid-ocean ridge, arc and intraplate. Irvine (1967) and Dick and Bullen

48 (1984) referred to the Cr# and Mg# of chromian spinel, and Arai (1994a, b) discussed

49 the relationship between the Cr# of chromian spinel and Fo of coexisting olivine in

50 peridotites and related rocks. The range of Cr# of chromian spinel alone, however, has

51 considerable overlaps between the different settings (Arai 1994a). The Mg# of chromian

52 spinel is strongly dependent on the equilibrium temperature (Irvine 1965; Jackson 1969),  
53 and is changeable at subsolidus stage also depending on its modal amount (Arai 1980).  
54 We should notice that the Mg#-Cr# relationship commonly used for descriptions and  
55 discussions of chromian spinel in igneous rocks (Irvine 1967) is strongly dependent on  
56 their subsolidus cooling histories after the igneous stage.

57 In this article, we review and summarize the chromian spinel chemistry (mainly the  
58 Cr# and Ti content) in deep-seated rocks (lherzolites, harzburgites, dunites, wehrlites,  
59 troctolites and gabbros) to define its chemical spread for discrimination of their tectonic  
60 settings and deep magmatic processes. We examined chromian spinel compositions in  
61 the ultramafic and mafic plutonic rocks (mantle peridotites and ultramafic/mafic  
62 cumulates) for which derived tectonic settings are well constrained. Each of the three  
63 settings, i.e., the mid-ocean ridge, arc (mantle wedge) and oceanic hotspot (intraplate),  
64 produces the magmas that are distinguishable from those of the other settings in  
65 geochemistry (e.g. Pearce 1975). There have been plenty of articles dealing with  
66 ultramafic xenoliths from continental areas captured by intra-plate basalts. The  
67 deep-seated rocks from non-arc continental areas are not used in this article, because  
68 they may have complicated histories, i.e., multi-setting generation/modification, and are

69 not appropriate to the purpose of this study. The chromian spinel chemistry has been  
70 systematically discussed both for mantle peridotites (e.g. Dick & Bullen 1984; Arai  
71 1994a) and for volcanic rocks (e.g. Arai, 1992; Kamenetsky *et al.* 2001). No works has  
72 ever discussed chromian spinel in possibly cumulative plutonic rocks (dunites, wehrlites,  
73 troctolites and gabbros) in more systematic way than this article that deals with  
74 chromian spinels from plutonic rocks only with well-constrained derivations. The result  
75 of this work is potentially useful, because such rocks are quite commonly found from  
76 various geologic bodies. We also present two examples of application of our result to  
77 two ophiolitic dunites, which are apparently unknown or debated for the tectonic setting  
78 of formation. This article is supplementary to Arai (1992), which deals with chromian  
79 spinels in volcanic rocks from the three tectonic settings.

80

## 81 DATA ACQUISITION

82 We collected data of chromian spinel in deep-seated rocks from three main tectonic  
83 settings, i.e., mid-ocean ridge, arc and oceanic hotspot. The source of spinel chemical  
84 data treated here is unpublished theses of our laboratory in addition to the literature.  
85  $\text{Fe}^{2+}$  and  $\text{Fe}^{3+}$  amounts were calculated assuming spinel stoichiometry. Titanium is

86 assumed to form the ulvospinel component.

87

## 88 MID-OCEAN RIDGES

89 We can obtain deep-seated rocks (lherzolites, harzburgites, dunites, wehrlites, troctolites

90 and gabbros) from the present-day ocean floor by dredging, drilling and submersible

91 diving (e.g. Dick 1989). The oceanic fracture zones (FZ), which are more prominently

92 developed in the slow to ultraslow spreading ridge systems than in fast spreading ones,

93 are the main loci for obtaining abyssal deep-seated rocks. Hess Deep, the East Pacific

94 Rise, is one of the non-FZ localities where deep-seated rocks are exposed on the ocean

95 floor (e.g. Arai & Matsukage 1996; Dick & Natland 1996; Allan & Dick 1996). We can

96 interpret these plutonics as deep-seated magmatic products beneath the mid-ocean ridge.

97 Harzburgites and lherzolites are predominant in the uppermost mantle of fast spreading

98 ridges and of slow spreading ridges, respectively (Niu & Hékinian 1997). Dunites and

99 related rocks (troctolites and olivine gabbros) are commonly found from Hess Deep,

100 and they may represent the Moho transition zone of the fast spreading ridge (e.g. Arai &

101 Matsukage 1996).

102

## 103 OPHIOLITES

104 Plutonic rocks from ophiolites may represent the deep-seated rocks of some sorts of  
105 oceanic lithosphere (e.g. Coleman 1977; Nicolas 1989). Their tectonic setting for  
106 genesis has been a problem in controversy since the pioneering paper of Miyashiro  
107 (1973), and therefore, the data from ophiolitic plutonic rocks are not considered in this  
108 section. Some ophiolites that exhibit both mid-ocean ridge and island-arc characteristics  
109 are called “supra-subduction zone” (SSZ) ophiolites (Pearce *et al.* 1984). Many people  
110 have favored the back-arc basin as the locus of the SSZ ophiolite formation (e.g. Pearce  
111 *et al.* 1984; Moores *et al.* 1984). The polygenetic nature of some ophiolites has been  
112 recently recognized as well. For example, some peridotites from the northern Oman  
113 ophiolite are of arc origin (e.g. Tamura & Arai 2006; Arai *et al.* 2006), although the  
114 main portion of the mantle section was of mid-ocean ridge origin (e.g. Nicolas 1989).  
115 Wehrlitic rocks around the Moho transition zone were interpreted as mid-ocean ridge  
116 products in the southern Oman ophiolite (Koga *et al.* 2001). For another example, the  
117 mantle member of the Coast Range ophiolite, California, is composed of a mixture of  
118 SSZ harzburgites and abyssal lherzolites (Choi *et al.* 2008; Jean *et al.* 2010).

119



## 120 ARCS

121 Deep-seated rocks from the sub-arc mantle (mantle wedge) are more difficult to obtain  
122 systematically. Alkali basalts that carry deep-seated rocks as xenoliths most frequently  
123 erupt on non-arc regions, i.e., on continental rift zones or oceanic hotspots, and the  
124 xenoliths in kimberlites represent the upper mantle beneath cratons (e.g. Nixon 1987).  
125 Genesis of calc-alkaline magmas is related with the subduction of slab (e.g. Tatsumi &  
126 Eggins 1995), and their deep-seated xenoliths undoubtedly represent the sub-arc  
127 deep-seated materials. Calc-alkaline andesites and basaltic andesites from Megata and  
128 Oshima-Ôshima volcanoes (Northeast Japan arc), Iraya volcano (Luzon arc), and  
129 Avacha and Shiveluch volcanoes (Kamchatka arc) contain peridotite xenoliths that are  
130 derived from lithosphere of the mantle wedge (e.g. Takahashi 1978; Ninomiya & Arai  
131 1992; Arai *et al.* 2003, 2004; Ishimaru *et al.* 2007; Bryant *et al.* 2007). It is noteworthy  
132 that some of ultramafic rocks treated here form composite xenoliths with gabbros and  
133 hornblendites in calc-alkaline volcanics (e.g. Ninomiya & Arai 1992; Arai *et al.* 1996,  
134 2003, 2004). A variety of peridotites, i.e. lherzolites to highly refractory harzburgites  
135 (Cr# of spinel < 0.8), may constitute the mantle wedge (Arai 1994a; Arai *et al.* 2003;  
136 Arai & Ishimaru 2008). Dunites and related rocks form a thick cumulus mantle beneath

137 the Southwest Japan arc (Takahashi 1978). Dunites are relatively abundant from the  
138 Oshima-Ôshima volcano (e.g. Yamamoto 1984), and are small in amount in other  
139 localities (especially the Megata, Iraya and Avacha volcanoes).

140 Although not treated here, we can obtain large amounts of ultramafic xenoliths  
141 carried by non-arc type alkaline basalts on past or present-day arcs, e.g., the Japan arcs  
142 (e.g. Takahashi 1978; Aoki 1987; Abe *et al.* 1998, 1999; Arai *et al.* 1998, 2000, 2007).

143 These materials from the Japan arcs may represent sub-arc mantle materials because  
144 their eruption ages are mostly younger than Miocene (Uto 1990), when the present arc  
145 setting had been established for the Japan island arcs (e.g. Otofuji *et al.* 1985).

146 Ultramafic to mafic xenoliths from the Southwest Japan arc have been affected to  
147 various extents (Arai *et al.* 2000) by Cenozoic non-arc type alkali basalt magmas  
148 (Nakamura *et al.* 1987).

149 Peridotites and related rocks are exposed on the ocean floor of fore-arc regions (e.g.  
150 Fisher & Engel 1969), and the dredged and drilled peridotites distinctively represent  
151 fore-arc mantle materials (e.g. Bloomer 1983; Parkinson & Pearce 1998). Refractory  
152 harzburgites are dominant in the fore-arc mantle (Arai 1994a). In this article, we treat  
153 only these two sets of deep-seated rocks, i.e., the ultramafic xenoliths in arc-type

154 volcanics and the ultramafic rocks exposed on the present-day fore-arc ocean floor, as  
155 “genuine” sub-arc materials with well-defined derivations.

156

## 157 OCEANIC HOTSPOTS

158 Deep-seated rocks from the oceanic hotspot areas have been almost solely obtained as  
159 ultramafic and mafic xenoliths in their volcanic rocks (e.g. Nixon 1987). The xenoliths  
160 in alkaline basalts especially represent the lower crust to upper mantle of that tectonic  
161 setting because the xenolith-bearing magmas postdate the main stage of hotspot  
162 volcanism (e.g. Jackson & Wright 1970). Lherzolites are apparently dominant in amount  
163 as the upper mantle material from the oceanic hotspot (Arai 1994a). Some peridotites  
164 may be related with the hotspot magmatism (cumulates or restites), and the others are  
165 only representative of the sub-oceanic mantle that hosts mantle plumes relevant to the  
166 hotspot activity. Arai (1994b) predicted predominance of refractory harzburgites with  
167 high Cr# (around 0.7) of chromian spinel as residual peridotites after the hotspot  
168 tholeiite genesis. Some basalt magmas contain a large amount of dunite xenoliths,  
169 indicating a thick dunite layer at the uppermost mantle as a result of extensive tholeiitic  
170 magmatism (Jackson & Wright 1970; Sen & Presnall 1986). Hawaiian and French

171 Polynesian hotspots are especially important for occurrences of ultramafic xenoliths

172 (Nixon 1987), and our data accumulation owes the literature dealing with them.

173

174 CHEMICAL SPECTRA OF CHROMIAN SPINELS IN PLUTONIC

175 ROCKS FROM THE THREE TECTONIC SETTINGS

176

177 MID-OCEAN RIDGES

178 As is well known, the Cr# of chromian spinel in abyssal mantle peridotites ranges from

179 0.1 to 0.6 (e.g. Dick & Bullen 1984; Arai 1994a; Niu & Hékinian 1997) (Fig. 1a). It

180 changes from around 0.4 to 0.6 in harzburgites to <0.4 in lherzolites, in response to a

181 decrease of degrees of partial melting (e.g. Dick & Bullen, 1984; Arai 1994a). The TiO<sub>2</sub>

182 content is mostly lower than 0.3 wt% in their chromian spinel (Fig. 1a). The chromian

183 spinel interestingly displays the same range of Cr# between plagioclase-bearing and

184 –free varieties of mantle peridotites (Fig. 1a). The TiO<sub>2</sub> content of chromian spinel is,

185 however, systematically higher in the plagioclase-bearing peridotites than in the

186 plagioclase-free ones (Dick 1989). The chromian spinel exhibits relatively wide ranges

187 of Cr#, 0.2-0.6, and TiO<sub>2</sub>, nil to 2 wt% (mostly <1 wt%) in abyssal dunites (Fig. 1a).

188 Other plutonic rocks, especially troctolites and olivine gabbros from Hess Deep, show a  
189 narrow range of Cr#, mostly 0.5 to 0.6, and a wide range of TiO<sub>2</sub> content, <3 wt% in  
190 chromian spinel. Chromian spinel in abyssal plutonic rocks is characterized by overall  
191 low Fe<sup>3+</sup> contents as that in MORB (Arai 1992). The Mg# is negatively correlated with  
192 the Cr# in chromian spinel for all peridotitic rocks including dunites from the mid-ocean  
193 ridges (Fig. 3a). Y<sub>Fe</sub> (= Fe<sup>3+</sup>/(Cr + Al + Fe<sup>3+</sup>) atomic ratio) of chromian spinel is mostly  
194 lower than 0.1 in peridotitic rocks, and lower than 0.2 in troctolites and gabbros (Figs.  
195 2a and 4a). Chromian spinel shows lower Mg#s at a Cr# around 0.5 in abyssal gabbros  
196 and troctolites. The TiO<sub>2</sub> content is well correlated positively with the Y<sub>Fe</sub> in chromian  
197 spinel from troctolites and gabbros, being 2.5 to 3 wt% at around Y<sub>Fe</sub> of 0.2 (Fig. 4a).

198       Rocks of dunite-troctolite-olivine gabbro suite from Hess Deep, East Pacific Rise,  
199 were interpreted as a reaction product between the primary MORB and mantle  
200 harzburgite (Arai & Matsukage 1996; Dick & Natland 1996). These rocks are expected  
201 to be in equilibrium with MORB in terms of mineral chemistry (e.g. Kelemen *et al.*  
202 1995; Arai 2005). Plagioclase in the harzburgites/lherzolites is calcic, and is a  
203 melt-impregnation product (e.g. Dick 1989). The formation of plagioclase-bearing  
204 peridotites is the very initiation of melt/peridotite reaction. The slightly but clearly

205 higher TiO<sub>2</sub> content of chromian spinel in plagioclase-bearing peridotites (Fig. 1a) is  
206 consistent with this interpretation (e.g. Dick 1989).

207

## 208 ARCS

209 The Cr# of chromian spinel exhibits a wide range, from than <0.2 to 0.9, for mantle  
210 peridotites (lherzolite to harzburgite) and dunites (Fig. 1b). This is consistent with the  
211 wide range of spinel Cr# in sub-arc mantle restites estimated from arc magmas (Arai  
212 1994b). The TiO<sub>2</sub> content of chromian spinel is, however, slightly higher in dunites than  
213 in mantle peridotites (Fig. 1b). Some of dunite, wehrlite and clinopyroxenite treated  
214 here possibly have initially formed composite xenoliths with younger gabbros or  
215 hornblendites, and have been chemically influenced by evolved magmas that formed the  
216 latter younger rocks (e.g. Ninomiya & Arai 1992). The relatively high contents of TiO<sub>2</sub>  
217 and Fe<sup>3+</sup> of some plutonic spinels are possibly due to such a secondary effect. Almost all  
218 sub-arc spinels have low values of Y<sub>Fe</sub>, < 0.3 (Fig. 2b). As is well known, the Mg#  
219 shows roughly negative correlations with the Cr# (e.g. Irvine 1967; Dick & Bullen  
220 1984) (Fig. 3b). Two Mg#-Cr# spinel trends can be recognized in mantle peridotites,  
221 especially harzburgites, corresponding to two different derivations of the samples

222 treated here, namely the fore-arc rocks and xenoliths in arc magmas (Fig. 3b). This is  
223 due to the difference of equilibrium temperature between the two rock suites (e.g.  
224 Okamura *et al.* 2006), resulting from a decrease of Mg# of chromian spinel with  
225 decreasing the equilibrium temperature in peridotites (Irvine 1967; Evans & Frost 1975).  
226 Chromian spinel in some dunites, wehrlites and clinopyroxenites shows lower Mg#s at  
227 given Cr#s (Fig. 3b). The TiO<sub>2</sub> content is positively correlated with the Fe<sup>3+</sup> ratio for the  
228 main cluster of sub-arc spinels, being 1 to 2 wt% at Y<sub>Fe</sub> = 0.2 (Fig. 4b).

229

### 230 OCEANIC HOTSPOTS (PLUMES)

231 Ultramafic xenoliths have been extensively described from various oceanic hotspots on  
232 the Earth, especially from Hawaii and the French Polynesian (e.g. Nixon 1987). The  
233 Cr# of chromian spinel also changes from 0.1 to 0.8 with a lithological change from  
234 lherzolite to harzburgite (Fig. 1c). The TiO<sub>2</sub> content of the peridotite spinel is mostly  
235 lower than 4 wt% (Fig. 1c). The Cr# of chromian spinel shows almost the same range  
236 between the mantle peridotites and dunites. The TiO<sub>2</sub> content of spinel is generally  
237 higher in dunites than in mantle peridotites, and show the highest values, up to > 10  
238 wt%, at the Cr# around 0.5 to 0.6 (Fig. 1c). Most of wehrlite spinel have relatively high

239 Cr#, around 0.6, and TiO<sub>2</sub> content, up to 6 wt% (Fig. 1c). The Y<sub>Fe</sub> of chromian spinel is  
240 highest around the intermediate Cr#, 0.5 to 0.6, and positively correlated to the TiO<sub>2</sub>  
241 content (Figs. 2c and 4c). The TiO<sub>2</sub> content of hotspot spinels varies at a given Y<sub>Fe</sub>,  
242 ranging from 1 to 6 wt% at Y<sub>Fe</sub> = 0.2 (Fig. 4c). Harzburgite spinels have higher Mg# at  
243 a given Cr# than dunite ones (Fig. 3c). As in the case of abyssal plutonic rocks, the Mg#  
244 is extended toward lower values at the highest Cr# of the whole range, 0.6 to 0.7, in the  
245 dunite spinels (Fig. 3c).

246

## 247 DISCUSSION

248

### 249 DISTINCTION OF THE THREE TECTONIC SETTINGS

250 Apart from the mantle peridotite, the plutonic rocks that bear chromian spinel are  
251 mainly dunite, troctolite and olivine gabbro from the ocean floor, but are dunite and  
252 wehrlite from the arc and the hotspot (Figs. 1 to 4). This indicates that the phase  
253 crystallizing next to olivine is mainly plagioclase in MORB but clinopyroxene in both  
254 arc and intraplate magmas. This is in turn related with the degree of partial melting in  
255 the mantle, which is lower, on average, in the mid-ocean ridge than in sub-arc and in



256 hotspot conditions (e.g. Arai 1994a,b).

257       The Cr# ranges of chromian spinel in plutonic rocks are overlapping with each  
258 other around 0.1 to 0.6 for the three tectonic settings, i.e., the mid-ocean ridge, arc and  
259 intraplate (Fig. 1). It is difficult, therefore, to distinguish the tectonic settings in terms of  
260 Cr# of spinel alone. The Cr# of spinel is barely higher than 0.6 in plutonic rocks from  
261 the mid-oceanic ridges. It is frequently over 0.6, and is up to 0.9 for the arc setting, and  
262 up to over 0.7 for the intraplate (hotspot or plume) setting. The TiO<sub>2</sub> content in  
263 chromian spinel combined with the Cr# is, however, convenient for distinction of  
264 plutonic rocks between the three tectonic settings (Fig. 1). The TiO<sub>2</sub> content of  
265 chromian spinel in plutonic rocks decreases on average from the intraplate setting to arc  
266 via mid-ocean ridge setting (Fig. 1). It is concluded that deep-seated ultramafic rocks  
267 can be distinguished as a group with each other in terms of spinel chemistry, especially  
268 Cr# and Ti content (Fig. 1). This distinction is consistent with the diversity of chromian  
269 spinel in volcanics depending on the tectonic setting (Arai 1992).

270

## 271 IMPLICATIONS FOR DEEP MAGMATIC PROCESSES

272 All kinds of plutonic rock have relatively low-Ti spinels from the arc setting, and

273 dunites are almost indistinguishable from harzburgites (or lherzolites) in terms of spinel  
274 chemistry (see Arai 1994b). Chromian spinel in dunites, troctolites and  
275 melt-impregnated harzburgites (plagioclase harzburgites) from the ocean floor is high  
276 both in Cr# (around 0.6 to 0.7) and in TiO<sub>2</sub> (Fig. 1a). Dunites and wehrlites from the  
277 oceanic hotspot also contain high-Cr# and high-Ti chromian spinels (Fig. 1c). The wide  
278 range of TiO<sub>2</sub> content at a given Y<sub>Fe</sub> for hotspot dunite spinels (Figs. 1 and 4) is possibly  
279 due to a variety of dunites, from those related with older MORB genesis to those related  
280 to younger hotspot magmatism. It is noteworthy that the hotspot plutonic spinels are  
281 lower in Ti at a given Y<sub>Fe</sub> than the mid-ocean ridge ones (Fig. 4), despite that the  
282 relations are the reverse for volcanic spinels (Arai 1992). Abyssal plutonic rocks are  
283 mostly troctolites (Fig. 4a), in which Ti and Fe<sup>3+</sup> are partitioned to chromian spinel  
284 because plagioclase is free of these components. In contrast, Ti and Fe<sup>3+</sup> are partitioned  
285 to both clinopyroxene and chromian spinel in wehrlites, which are common from  
286 hotspot environments (Fig. 4c). This is also related with the redox condition;  
287 deep-seated magmas are more oxidized for the hotspot environments than for the  
288 mid-ocean ridge ones. This is concordant to the difference of oxidation states between  
289 the hotspot magmas and MORB (e.g. Christie *et al.* 1986; Rhodes & Vollinger 2005).

290       Discrepancy in spinel chemistry between effusive rocks and related plutonic rocks  
291 is sometimes noticeable; volcanic spinels are sometimes more limited in Ti and  $Y_{Fe}$   
292 ranges than plutonic spinels (Fig. 4). This is primarily due to effective magmatic  
293 evolution to concentrate these components within closed melt pools in deep parts (Arai  
294 *et al.* 1997). Difference in spinel chemistry is striking between MORB and abyssal  
295 plutonics (dunites, troctolites to olivine gabbros) (Fig. 4a). The  $TiO_2$  and  $Y_{Fe}$  of  
296 chromian spinel are limited, mostly <1 wt% and <0.1, respectively in MORB (Arai  
297 1992), as compared to the values in abyssal plutonics (Fig. 4a).

298       It is noteworthy that high-Ti chromian spinels are also high in Cr# (around 0.6 to  
299 0.7) (Fig. 1). The high-Cr#, -Ti spinels are common to dunites and related rocks from  
300 the ocean floor and oceanic hotspot, part of which have been thought to be  
301 peridotite/magma reaction products (e.g. Arai & Matsukage 1996; Dick & Natland  
302 1996). Some of dunite and wehrlite xenoliths from the island arc setting are also  
303 reaction products (e.g. Arai & Abe 1994), but the concerned arc magmas, which are  
304 initially low-Ti, have not increased the Ti contents of chromian spinel even through the  
305 peridotite/melt reaction processes.

306

## 307 EXAMPLES OF APPLICATION TO OPHIOLITES

308 The origin and nature of ophiolites have been controversial (e.g. Pearce *et al.* 1984;  
309 Nicolas 1989). Arai *et al.* (2006), for example, suggested polygenetic nature of the  
310 mantle part of the northern Oman ophiolite. We show two examples of discordant  
311 dunites from two ophiolites as below. The dunite is an important constituent of the  
312 Moho transition zone to upper mantle section of ophiolites, but the mineralogy is too  
313 simple to constrain its derivation. If we apply the systematics discussed here, the  
314 chromian spinel is indicative of the tectonic setting of the dunite formation.

315

## 316 DISCORDANT DUNITES FROM THE MANTLE SECTION OF THE

## 317 NORTHERN OMAN OPHIOLITE

318 It has been well recognized that the mantle section of the Oman ophiolite is dominated  
319 by harzburgites (e.g. Boudier & Coleman 1981; Lippard *et al.* 1986). Lherzolites are  
320 absent except at the base of the ophiolite (e.g. Lippard *et al.* 1986; Takazawa *et al.*  
321 2003). The harzburgites mainly constitute the mantle section, containing spinels with  
322  $Cr\#s < 0.6$  (Le Mée *et al.* 2004), similar to those obtained from the ocean floor of fast  
323 spreading ridge origin (Niu & Hekinian 1997). Tamura and Arai (2006) found a

324 harzburgite-orthopyroxenite-dunite suite of sub-arc chemical affinity from the northern  
325 Oman ophiolite. Arai *et al.* (2006) examined chemical variations of detrital chromian  
326 spinel particles derived from the mantle section from recent riverbeds in the Oman  
327 ophiolite. They found more than 20 to 30 percent of the total detrital chromian spinel  
328 grains examined have Cr#s higher than 0.6 (Arai *et al.* 2006).

329       Discordant dunites cutting foliated harzburgites are very common in the mantle  
330 section (Fig. 5a). They form dikes or networks, and some of them contain chromian  
331 spinel concentrations (podiform chromitites) (e.g. Augé 1987; Ahmed & Arai 2002).  
332 They are massive in appearance and solely comprise olivine and euhedral to subhedral  
333 chromian spinel (Fig. 5b). We examined chromian spinels in the discordant dunites from  
334 Wadi Rajmi and Wadi Fizh areas of the northern Oman ophiolite (Fig. 5a). The Cr# of  
335 chromian spinel ranges from 0.4 to 0.8 with very low amounts of TiO<sub>2</sub>, mostly < 0.3  
336 wt% (Fig. 6). Olivine associated with the chromian spinel is around Fo<sub>90-92</sub> in  
337 composition. The Oman discordant dunites are most likely to have been related with arc  
338 magmas (see Figs. 1, 2 and 4). The mantle section of the Oman ophiolite, therefore,  
339 comprises the ocean-floor peridotites (mainly harzburgites) modified by addition of  
340 dunites of sub-arc affinity. This suggests a switch of tectonic setting from mid-ocean

341 ridge to arc (= supra-subduction zone) for genesis of the Oman ophiolite (Arai *et al.*  
342 2006). Alternatively, this characteristic can be obtained at a back-arc tectonic setting,  
343 where various magmas, from MORB-like to arc-type, are available (e.g. Pearce *et al.*  
344 1984).

345

#### 346 DISCORDANT DUNITES FROM THE LIZARD OPHIOLITE, CORNWALL

347 The mantle section of the Lizard ophiolite, Cornwall (Kirby 1979), is mainly composed  
348 of lherzolites and concordant dunites (Green 1964; Kadoshima & Arai 2001). This is  
349 very similar to a peridotite suite from the ocean floor of slow spreading ridge origin  
350 (Roberts *et al.* 1993) if we consider the abundance of lherzolite over harzburgite (e.g.  
351 Niu & Hekinian 1997). The Cr# ranges from 0.1 to 0.5 for the Lizard detrital spinels  
352 (Kadoshima & Arai 2001), exactly being the same as those of abyssal peridotites  
353 (lherzolites to harzburgites) (Fig. 6). This is consistent with the idea that the Lizard  
354 peridotite was representative of the uppermost sub-oceanic mantle of a slow spreading  
355 ridge, which may be composed of predominant lherzolites and subordinate harzburgites  
356 (Arai 2005).

357 Networks of younger discordant dunites are prominently cutting the concordant

358 lherzolites and dunites, especially around the central part of the ophiolite (Kadoshima &  
359 Arai 2001). The younger discordant dunites are black in hand specimen, and seem  
360 compact and hard on outcrop (Fig. 5c). This is in contrast to the concordant dunites that  
361 are severely altered/weathered to be pale green in color and have been more strongly  
362 eroded than the discordant ones due to mechanical weakness. This observation clearly  
363 indicates different chemical and/or textural characteristics between the two types of  
364 dunite. The discordant dunites are exclusively composed of olivine, highly serpentinized,  
365 and euhedral to subhedral chromian spinel. The chromian spinel is opaque in thin  
366 section and contains minute exsolution blebs of a Ti-rich phase (possibly Ti-rich  
367 magnetite) (Fig. 5d). The olivine shows slightly lower Fo contents, 83 to 88, than in the  
368 wall peridotite (89-90). The chromian spinel of this younger dunite is high in Cr# and  
369 TiO<sub>2</sub>, being around 0.6 and up to > 4 wt%, respectively (Fig. 6). It is low in both Cr#  
370 and TiO<sub>2</sub> near the boundary with lherzolite (Fig. 6), suggesting fractional crystallization  
371 (precipitation of minerals from the wall inward) or a reaction between the involved melt  
372 and the lherzolite. The primary chromian spinel in the discordant dunite should have  
373 contained higher TiO<sub>2</sub> contents before unmixing of the Ti-rich phase, being within the  
374 chemical range of dunite spinels from oceanic hotspots (see Figs. 1 and 2). The magma

375 that produced the discordant dunite within the Lizard peridotite was of hotspot  
376 (intra-plate) origin (Figs. 1, 2, 4 and 6). It was most probably tholeiitic (cf. Arai 1992).  
377 The Lizard peridotite was, therefore, derived from the uppermost mantle that was  
378 initially generated at a slow spreading ridge and was later impacted by an intra-plate  
379 tholeiite magma.

380

## 381 CONCLUSIONS

382 The chromian spinel chemistry is highly useful to petrologically characterize ultramafic  
383 plutonic rocks, especially dunitic rocks and chromitites, where chromian spinel is often  
384 the only discriminating mineral. The trivalent cation ratio and  $\text{TiO}_2$  content in chromian  
385 spinel are important parameters in discrimination of the plutonic rocks in terms of  
386 tectonic setting of formation. Discrimination diagrams based on spinel chemistry made  
387 from plutonic rocks derived from well-constrained settings should be applied to  
388 characterization of rocks from unknown origins. The spinel-based diagrams made for  
389 volcanic rocks or magmas should not been used for discrimination of plutonic rocks in  
390 tectonic setting of derivation, because chromian spinel shows different chemical ranges  
391 between effusive and plutonic rocks even of the same magmatic affinity as discussed



392 above. Discrimination in Mg# of chromian spinel is sometimes unreliable, because the  
393 Mg# in chromian spinel is strongly changeable depending on the thermal history in  
394 olivine-rich rocks. For example, the chromian spinel in possible abyssal peridotites  
395 suffered from low-temperature metamorphism at a subduction zone have lower Mg#s at  
396 a given Cr# than abyssal peridotites from the present-day ocean floor, which are mostly  
397 derived from near the spreading center and have not been cooled down sufficiently (e.g.  
398 Hirauchi *et al.* 2008).

399

#### 400 ACKNOWLEDGEMENTS

401 We are grateful to T. Morishita and A. Ishiwatari for their discussions. S.A. thanks H.  
402 Hirai, N. Abe, M. Kida, Y. Kobayashi, M. Fujiwara, Y. Saeki, A. Ninomiya, S. Takada,  
403 N. Takahashi and K. Goto for their collaboration on mantle xenoliths derived from the  
404 mantle wedge. We appreciate suggestions made by S.H. Choi (associate editor), Y.J. Yu  
405 and J.W. Shervais, which were helpful in revision.

406

#### 407 REFERENCES

408 ABE N., ARAI S. & SAEKI Y. 1992. Hydration processes in the arc mantle; petrology

- 409 of the Megata peridotite xenolith the Northeast Japan arc. *Journal of Mineralogy,*  
410 *Petrology and Economic Geology* **87**, 305-17. (in Japanese with English abstract)
- 411 ABE N., ARAI S. & NINOMIYA A. 1995. Peridotite xenoliths and essential ejecta from  
412 the Ninomegata crater, the Northeastern Japan arc. *Journal of Mineralogy, Petrology*  
413 *and Economic Geology* **90**, 41-9. (in Japanese with English abstract)
- 414 ABE N., ARAI S. & YURIMOTO H. 1998. Geochemical characteristics of the  
415 uppermost mantle beneath the Japan island arcs: implications for upper mantle  
416 evolution. *Physics of Earth and Planetary Interior* **107**, 233-47.
- 417 ABE N., ARAI S. & YURIMOTO H. 1999. Texture-dependent geochemical variations  
418 of sub-arc mantle peridotite from Japan island arcs. *Proceedings of VIIth*  
419 *International Kimberlite Conference J.B. Dawson Vol.*, 13-22.
- 420 AHMED A.H. & ARAI S. 2002. Unexpectedly high-PGE chromitite from the deeper  
421 mantle section of the northern Oman ophiolite and its tectonic implications.  
422 *Contributions to Mineralogy and Petrology* **143**, 263-78.
- 423 ALLAN J.F. & DICK H.J.B. 1996. Cr-rich spinel as a tracer for melt migration and  
424 melt-wall rock interaction in the mantle: Hess Deep, Leg 147. *Proceedings of ODP,*  
425 *Scientific Results* **147**, 157-72.

- 426 AOKI K. 1987. Japanese Island arc: xenoliths in alkali basalts, high-alumina basalts,  
427 and calc-alkaline andesites and dacites. *In* Nixon P.H. (ed.) *Mantle Xenoliths*, pp  
428 314-331, John Wiley & Sons, New York.
- 429 ARAI S. 1980. Dunite-harzburgite-chromitite complexes as refractory residue in the  
430 Sangun-Yamaguchi zone, western Japan. *Journal of Petrology* **21**, 141-65.
- 431 ARAI S. 1992. Chemistry of chromian spinel in volcanic rocks as a potential guide to  
432 magma chemistry. *Mineralogical Magazine* **56**, 173-84.
- 433 ARAI S. 1994a. Characterization of spinel peridotites by olivine-spinel compositional  
434 relationships: Review and interpretation. *Chemical Geology* **113**, 191-204.
- 435 ARAI S. 1994b. Compositional variation of olivine-chromian spinel in Mg-rich  
436 magmas as a guide to their residual spinel peridotites. *Journal of Volcanology and*  
437 *Geothermal Research* **59**, 279-94.
- 438 ARAI S. 2005. Role of dunite in genesis of primitive MORB. *Proceedings of Japan*  
439 *Academy. Series B* **81**, 14-9.
- 440 ARAI S. & ABE N. 1994. Podiform chromitite in the arc mantle: chromitite xenoliths  
441 from the Takashima alkali basalt, southwest Japan arc. *Mineralium Deposita* **29**,  
442 434-8.

- 443 ARAI S., ABE N. & HIRAI H. 1998. Petrological characteristics of the sub-arc mantle:  
444 an overview on petrology of peridotite xenoliths from the Japan arcs. *Trends in*  
445 *Mineralogy (India)* **2**, 39-55.
- 446 ARAI S., ABE N. & ISHIMARU S. 2007. Mantle peridotites from the Western Pacific.  
447 *Gondwana Research*, **11**, 180-99.
- 448 ARAI S., HIRA H. & UTO K. 2000. Mantle peridotite xenoliths from the Southwest  
449 Japan arc and a model for the sub-arc upper mantle structure and composition of the  
450 Western Pacific rim. *Journal of Mineralogical and Petrological Sciences* **95**, 9-23.
- 451 ARAI S. & ISHIMARU S. 2008. Insights into petrological characteristics of the  
452 lithosphere of mantle wedge beneath arcs through peridotite xenoliths: A review.  
453 *Journal of Petrology* **49**, 665-95.
- 454 ARAI S., ISHIMARU S. & OKRUGIN V.M. 2003. Metasomatized harzburgite  
455 xenoliths from Avacha volcano as fragments of mantle wedge of the Kamchatka arc:  
456 an implication for the metasomatic agent. *Island Arc* **12**, 233-46.
- 457 ARAI S., KADOSHIMA K. & MORISHITA T. 2006. Widespread arc-related melting in  
458 the mantle section of the northern Oman ophiolite as inferred from detrital chromian  
459 spinels. *Journal of Geological Society, London* **163**, 869-79 .

- 460 ARAI S., KIDA M., ABE N., NINOMIYA A. & YUMUL G.P. JR. 1996. Classification  
461 of peridotite xenoliths in calc-alkaline andesite from Iraya volcano, Batan Island, the  
462 Philippines, and its genetical implications. *Science Reports of Kanazawa University*  
463 **41**, 25-45.
- 464 ARAI S. & MATSUKAGE K. 1996. Petrology of the gabbro-troctolite-peridotite  
465 complex from Hess Deep, equatorial Pacific: implications for mantle-melt  
466 interaction within the oceanic lithosphere. *Proceedings of ODP, Scientific Results*  
467 **147**, 135-55.
- 468 ARAI S., MATSUKAGE K., ISOBE E. & VYSOTSKIY S. 1997. Concentration of  
469 incompatible elements in oceanic mantle: Effect of melt/wall interaction in stagnant  
470 or failed conduits within peridotite. *Geochimica et Cosmochimica Acta* **61**, 671-175.
- 471 ARAI S., TAKADA S., MICHIBAYASHI K. & KIDA M. 2004. Petrology of peridotite  
472 xenoliths from Iraya Volcano, Philippines, and its implication for dynamic  
473 mantle-wedge processes. *Journal of Petrology* **45**, 369-89.
- 474 AUGÉ T. 1987. Chromite deposits in the northern Oman ophiolite: mineralogical  
475 constraints. *Mineralium Deposita*, **109** 301-4.
- 476 BARSDLELL M & SMITH I.E.M. 1989. Petrology of recrystallized ultramafic xenoliths

- 477 from Merelava volcano, Vanuatu. *Contributions to Mineralogy and Petrology* **102**,  
478 230-41.
- 479 BLOOMER S.H. 1983. Distribution and origin of igneous rocks from the landward  
480 slopes of the Mariana Trench; Implications for its structure and evolution. *Journal of*  
481 *Geophysical Research* **88**, 7411-28.
- 482 BLOOMER S.H. & FISHER R.L. 1987. Petrology and geochemistry of igneous rocks  
483 from the Tonga trench — A non-accreting plate boundary. *Journal of Geology* **95**,  
484 469-95.
- 485 BLOOMER S.H. & HAWKINS J.W. 1983. Gabbroic and ultramafic rocks from the  
486 Mariana Trench: An island arc ophiolite. In Hayes D.E. (ed.) *The tectonic and*  
487 *geologic evolution of southeast Asian seas and Islands (Part 2)*, pp 294-317,  
488 Geophysical Monograph No. 27, American Geophysical Union, Washington, D.C..
- 489 BOUDIER F. & COLEMAN R.G. 1981. Cross section through the peridotite in the  
490 Samail ophiolite, southeastern Oman mountains. *Journal Geophysical Research* **86**,  
491 2573-92.
- 492 BRYANT J.A., YOGODZINSKI G.M. & CHURIKOVA T.G. 2007. Melt-mantle  
493 interaction beneath the Kamchatka arc: Evidence from ultramafic xenoliths from

- 494 Shiveluch volcano. *Geochemistry, Geophysics, Geosystems* **8**, Q04007. doi:  
495 10.1029200GC001443.
- 496 CANNAT M., CHATIN F., WHITECHURCH H. & CEULENEER G. 1997. Gabbroic  
497 rocks trapped in the upper mantle at the mid-Atlantic ridge. *Proceedings of ODP,*  
498 *Scientific Results* **153**, 243-64.
- 499 CHOI S.H., SHERVAIS J.W. & MUKASA S.B. 2008. Supra-subduction and abyssal  
500 mantle peridotites of the Coast Range ophiolite, California. *Contributions to*  
501 *Mineralogy and Petrology* **156**, 551-576.
- 502 CHRISTIE D.M., CARMICHAEL I.S.E. & LANGMUIR C.H. 1986. Oxidation states  
503 of mid-ocean ridge basalt glasses. *Earth Planetary Science Letters* **79**, 397-411.
- 504 CLAGUE D.A. 1988. Petrology of ultramafic xenolith from Loihi seamount, Hawaii.  
505 *Journal of Petrology* **29**, 1161-86.
- 506 COLEMAN R.G. 1977. *Ophiolites*. Springer, Berlin.
- 507 CONRAD W.K. & KAY R.W. 1984. Ultramafic and mafic inclusions from Adak Island:  
508 crystallization history, and implications for the nature of primary magmas and  
509 crustal evolution in the Aleutian arc. *Journal of Petrology* **25**, 88-125.
- 510 DEBARI S., KAY S.M. & KAY R.W. 1987. Ultramafic xenoliths from Adagdak

- 511 volcano, Adak, Aleutian Islands, Alaska: deformed igneous cumulates from the  
512 Moho of an island arc. *Journal of Geology* **95**, 329-41.
- 513 DELONG S.E., HODGES F.N. & ARCULUS R.J. 1975. Ultramafic and mafic  
514 inclusions, Kanaga Island, Alaska, and the occurrence of alkaline rocks in island  
515 arcs. *Journal of Geology* **83**, 721-36.
- 516 DICK H.J.B. 1989. Abyssal peridotites, very slow spreading ridges and ocean ridge  
517 magmatism. In Saunders A.D. and Norry M.J. (eds.) *Magmatism in the Ocean*  
518 *Basins*, Geological Society Special Publications No. 42, pp 71-106, The Geological  
519 Society, London.
- 520 DICK H.J.B. & BULLEN T. 1984. Chromian spinel as a petrogenetic indicator in  
521 abyssal and alpine type peridotites and spatially associated lavas. *Contributions to*  
522 *Mineralogy and Petrology* **86**, 54-76.
- 523 DICK H.J.B. & NATLAND J. 1996. Last-stage melt evolution and transport in the  
524 shallow mantle beneath the East Pacific Ridge. *Proceedings of ODP, Scientific*  
525 *Results* **147**, 103-34.
- 526 EVANS B.W. & FROST B.R. 1975. Chrome-spinel in progressive metamorphism: A  
527 preliminary analysis. *Geochimica et Cosmochimica Acta* **39**, 959-72.



- 528 FISHER R.L. & ENGEL C.G. 1969. Ultramafic and basaltic rocks dredged from the  
529 nearshore flank of the Tonga trench. *Geological Society of America Bulletin* **80**,  
530 1373-78.
- 531 FUJII T. 1990. Petrology of peridotites from Hole 670A, Leg109. *Proceedings of ODP*,  
532 *Scientific Results* **106/109**, 19-25.
- 533 GREEN D.H. 1964. The petrogenesis of the high-temperature peridotite intrusion in the  
534 Lizard area, Cornwall. *Journal of Petrology* **5**, 134-88.
- 535 HIRAUCHI K., TAMURA A., ARAI S., YAMAGUCHI H. & HISADA K. 2008. Fertile  
536 abyssal peridotites within the Franciscan subduction complex, central California:  
537 possible origin as detached remnants of oceanic fracture zones located close to a  
538 slow-spreading ridge. *Lithos* **105**, 319-28.
- 539 IRVINE T.N. 1965. Chromian spinel as a petrogenetic indicator; part I, Theory.  
540 *Canadian Journal of Earth Sciences* **2**, 648-71.
- 541 IRVINE T.N. 1967. Chromian spinel as a petrogenetic indicator; part II, Petrologic  
542 applications. *Canadian Journal of Earth Sciences* **4**, 71-103.
- 543 ISHII T. 1985. Dredged samples from the Ogasawara fore-arc seamount or “Ogasawara  
544 Paleoland” – “fore-arc ophiolite”. In Nasu N., Kobayashi K., Uyeda S., Kushiro I.

- 545 and Kagami H. (eds.), *Formation of Active Ocean Margin*, pp 307-42, TERRAPUB,  
546 Tokyo.
- 547 ISHII T., ROBINSON P.T., MAEKAWA H. & Fiske R. 1992. Petrological studies of  
548 peridotites from diapiric serpentinite seamounts in the Izu-Ogasawra-Mariana  
549 forearc, Leg 125. *Proceedings of ODP, Scientific Results* **125**, 445-85.
- 550 ISHII T., SATO H., HARAGUCHI S., FRAYER P., FUJIOKA K., BLOOMER S. &  
551 YOKOSE H. 2000. Petrological characteristics of peridotites from serpentinite  
552 seamounts in the Izu-Ogasawara-Mariana forearc. *Journal of Geography (Tokyo)*  
553 **109**, 517-30. (in Japanese with English abstract)
- 554 ISHIMARU S. 2004. *The petrological characteristics of the mantle wedge beneath the*  
555 *Kamchatka arc*. Unpublished MSc thesis, Kanazawa University, Kanazawa.
- 556 ISHIMARU S., ARAI S., ISHIDA Y., SHIRASAKA M. & OKRUGIN V. M. 2007.  
557 Melting and multi-stage metasomatism in the mantle wedge beneath a frontal arc  
558 inferred from highly depleted peridotite xenoliths from the Avacha volcano,  
559 southern Kamchatka. *Journal of Petrology* **48**, 395-433.
- 560 JACKSON E.D. 1969. Chemical variation in co-existing chromite and olivine in  
561 chromite zones of the Stillwater complex. In H.D.B. Wilson H.D.B. (ed.) *Magmatic*

- 562 *Ore Deposits*, Economic Geology Monograph No. 6, pp 41-71, The Economic  
563 Geology Publishing Company, New Haven.
- 564 JACKSON E.D. & WRIGHT T.L. 1970. Xenoliths in the Honolulu Volcanic Series,  
565 Hawaii. *Journal of Petrology* **11**, 405-30.
- 566 JEAN M.M., SHERVAIS J.W., CHOI S.H. & MUKASA S.B. 2010. Melt extraction and  
567 melt refertilization in mantle peridotite of the Coast Range ophiolite: an La-ICP-MS  
568 study. *Contributions to Mineralogy and Petrology* **159**, 113-136.
- 569 KADOSHIMA K. & ARAI S. 2001. Chemical analysis of detrital chromian spinels  
570 from the Lizard area, Cornwall, England: an attempt for lithological and petrological  
571 survey of the Lizard peridotite. *Neues Jahrbuch für Mineralogie Monatshefte* **2001**,  
572 193-209.
- 573 KAMENETSKY V.S., CRAWFORD A.J. & MEFFRE S. 2001. Factors controlling  
574 chemistry of magmatic spinel: an empirical study of associated olivine, Cr-spinel  
575 and melt inclusions from primitive rocks. *Journal of Petrology* **42**, 655-71.
- 576 KELEMEN P.B., SHIMIZU N. & SALTERS V.J.M. 1995. Extraction of  
577 mid-ocean-ridge basalt from the upwelling mantle by focused flow of melt in dunite  
578 channels. *Nature* **375**, 747-753.

- 579 KIRBY G.A. 1979. The Lizard Complex as an ophiolite. *Nature* **282**, 58-61.
- 580 KOGA K.T., KELEMEN P.B. & SHIMIZU N. 2001. Petrogenesis of the crust-mantle  
581 transition zone and the origin of lower crustal wehrlite in the Oman ophiolite.  
582 *Geochemistry, Geophysics, Geosystems* **2**, 2000GC000132.
- 583 KOMOR S.C., GROVE T.L. & HÉBERT R. 1990. Abyssal peridotites from ODP Hole  
584 670A (21°10'N, 45°02'W): Residues of mantle melting exposed by non-constructive  
585 axial divergence. *Proceedings of ODP, Scientific Results* **106/109**, 85-101.
- 586 LE MÉE L., GIRARDEAU J. & MONNIER C. 2004. Mantle segmentation along the  
587 Oman ophiolite fossil mid-ridge. *Nature* **432**, 167-72.
- 588 LIPPARD S.J., SHELTON A.W. & GASS I.G. 1986. *The Ophiolite of Northern Oman*.  
589 Geological Society Memoir No. 11, Geological Society, London.
- 590 MIYASHIRO A. 1973. The Troodos ophiolitic complex was probably formed in an  
591 island arc. *Earth and Planetary Science Letters* **19**, 218-224.
- 592 MOORES E.M., ROBINSON P.T., MALPAS J. & XENOPHONTOS C. 1984. Model  
593 for origin of the Troodos massif, Cyprus, and other mideast ophiolites. *Geology* **12**,  
594 500-503.

- 595 NAKAMURA E., CAMPBELL I.H., McCULLOCH M.T. 1989. Chemical  
596 geodynamics in a back arc region around the Sea of Japan: implications for the  
597 genesis of alkaline basalts in Japan, Korea, and China. *Journal of Geophysical*  
598 *Research* **94**, 4634-4654.
- 599 NICOLAS A. 1989. *Structure of Ophiolites and Dynamics of Oceanic Lithosphere*.  
600 Kluwer, Dordrecht.
- 601 NIIDA K. 1997. Mineralogy of Mark peridotites: Replacement through magma  
602 channeling examined from Hole920D, MARK area. *Proceedings of ODP, Scientific*  
603 *Results* **153**, 265-75.
- 604 NINOMIYA A. & ARAI S. 1992. Harzburgite fragment in a composite xenolith from an  
605 Oshima-Oshima andesite, the Northeast Japan arc. *Bulletin of Volcanological*  
606 *Society of Japan* **37**, 269-73 (in Japanese).
- 607 NIU Y. & HÉKINIAN R. 1997. Spreading-rate dependence of the extent of mantle  
608 melting beneath ocean ridges. *Nature* **385**, 326-29.
- 609 NIXON P.H. 1987. *Mantle Xenoliths*. John Wiley & Sons, New York.
- 610 OHARA Y. & ISHII T. 1998. Peridotites from the southern Mariana forearc:  
611 Heterogeneous fluid supply in the mantle wedge. *Island Arc* **7**, 541-58.

- 612 OKAMURA H., ARAI S. & KIM Y.U. 2006. Petrology of forearc peridotite from the  
613 Hahajima Seamount, the Izu-Bonin arc, with special reference to chemical  
614 characteristics of chromian spinel. *Mineralogical Magazine* **70**, 15-26.
- 615 OTOFUJI Y., MATSUDA T. & NOHDA S. 1985. Paleomagnetic evidence from the  
616 Miocene counter-clockwise rotation of Northeast Japan – rifting process of the  
617 Japan Sea. *Earth and Planetary Science Letters* **75**, 265-77.
- 618 PARKINSON I.J. & PEARCE J.A. 1998. Peridotites from the Izu-Bonin-Mariana  
619 forearc (ODP Leg 125): Evidence for mantle melting and melt-mantle interaction in  
620 a supra-subduction zone setting. *Journal of Petrology* **39**, 1577-618.
- 621 PEARCE J.A. 1975. Basalt geochemistry used to investigate past tectonic environments  
622 on Cyprus. *Tectonophysics* **25**, 41-67.
- 623 PEARCE J.A., LIPPARD S.J. & ROBERTS S. 1984. Characteristics and tectonic  
624 significance of supra subduction zone ophiolites. In Kokelaar B.P. and Howells M.R.  
625 (eds.) *Marginal Basin Geology*, Geological Society Special Publications No. 16, pp  
626 77-94, The Geological Society, London.
- 627 PRINZ M., KEIL K., GREEN J.A., REID A.M., BONATTI E. & HONNOREZ J. 1976.  
628 Ultramafic and mafic dredge samples from the equatorial mid-Atlantic and fracture

- 629 zones. *Journal of Geophysical Research* **81**, 4087-103.
- 630 RHODES J.M. & VOLLINGER M.J. 2005. Ferric/ferrous ratios in 1984 Mauna Loa  
631 lavas: a contribution to understanding the oxidation state of Hawaiian magmas.  
632 *Contributions to Mineralogy and Petrology* **149**, 666-74.
- 633 ROBERTS S., ANDERS J.R., BULL J.M. & SANDERSON D.J. 1993. Slow-spreading  
634 ridge-axis tectonics: evidence from Lizard Complex, U.K. *Earth and Planetary  
635 Science Letters* **116**, 101-12.
- 636 ROEDER P.L. 1994. Chromite: From the fiery rain of chondrules to the Kilauea Iki lava  
637 lake. *Canadian Mineralogist* **32**, 729-46.
- 638 SEN G. & PRESNALL D.C. 1986. Petrogenesis of dunite xenoliths from Koolau  
639 volcano, Oahu, Hawaii: Implications for Hawaiian volcanism. *Journal of Petrology*  
640 **27**, 197-217.
- 641 TAKAHASHI E. 1978. Petrological model of the crust and upper mantle of the  
642 Japanese Island Arcs. *Bulletin Volcanologique* **41**, 529-47.
- 643 TAKAZAWA E., OKAYASU T. & SATOH K. 2003. Geochemistry and origin of the  
644 basal lherzolites from the northern Oman ophiolite (northern Fizeh block).  
645 *Geochemistry, Geophysics, Geosystems* **4**, 1021, doi:10.1029/2001GC000232.

- 646 TAMURA A. & ARAI S. 2006. Harzburgite-dunite-orthopyroxenite suite as a record of  
647 supra-subduction zone setting for the Oman ophiolite mantle. *Lithos* **90**, 43-56.
- 648 TANAKA C. 1999. *Upper mantle beneath hotspots inferred from peridotite xenoliths*.  
649 Unpublished MSc thesis, Kanazawa University, Kanazawa.
- 650 TARTAROTTI P., SUSINI S., NIMIS P. & OTTOLINI L. 2002. Melt migration in the  
651 upper mantle along the Romanche Fracture Zone (Equatorial Atlantic). *Lithos* **63**,  
652 125-49.
- 653 TATSUMI Y. & EGGINS S. 1995. *Subduction Zone Magmatism*. Blackwell,  
654 Cambridge.
- 655 TRACY R.J. 1980. Petrology and genetic significance of an ultramafic xenolith suite  
656 from Tahiti. *Earth and Planetary Science Letters* **48**, 80-96.
- 657 UTO K. 1990. Neogene volcanism of Southwest Japan: Its time and space on K-Ar  
658 dating. Ph.D. thesis, University of Tokyo, Tokyo.
- 659 YAMAMOTO M. 1984. Origin of calc-alkaline andesite from Oshima-Ōshima volcano,  
660 north Japan. *Journal of Faculty of Science, Hokkaido University, Series 4*, **21**, 1,  
661 77-131.
- 662
- 663



664 Figure Captions

665

666 Fig. 1. Relationships between  $\text{TiO}_2$  contents and  $\text{Cr}/(\text{Cr} + \text{Al})$  atomic ratios of  
667 chromian spinels in plutonic rocks. Upper and lower panels are for dunites and other  
668 possible cumulates, and for peridotites, respectively. (a) Mid-ocean ridges. Data  
669 source: Allan and Dick (1996), Arai and Matsukage (1996), Cannat *et al.* (1997),  
670 Dick (1989), Dick and Natland (1996), Fujii (1990), Niida (1997), Komor *et al.*  
671 (1990), Prinz *et al.* (1976), and Tartarotti *et al.* (2002). (b) Arcs. Data source: Abe *et*  
672 *al.* (1992, 1995), Arai *et al.* (2004), Barsdell and Smith (1989), Bloomer and  
673 Hawkins (1983), Bloomer and Fisher (1987), Conrad and Kay (1984), Debari *et al.*  
674 (1987), Delong *et al.* (1975), Ishii (1985), Ishii *et al.* (1992, 2000), Ishimaru (2004),  
675 Ninomiya and Arai (1992), Ohara and Ishii (1998), and Yamamoto (1984). (c)  
676 Oceanic hotspots. Data source: Clague (1988), Sen and Presnall (1986), Tracy  
677 (1980), and Tanaka (1999). Peridotites, lherzolites and harzburgites. Pl, plagioclase.  
678 Ol, olivine. Note the different compositional ranges between the three tectonic  
679 settings. Scales of vertical axis are different between (a) and (b), and (c).

680

681 Fig. 2. Cr-Al-Fe<sup>3+</sup> atomic relationships of chromian spinels in plutonic rocks. Right  
682 and left panels are for dunites and other possible cumulates, and for peridotites,  
683 respectively. (a) Mid-ocean ridges. (b) Arcs. (c) Oceanic hotspots. Peridotites,  
684 lherzolites and harzburgites. Pl, plagioclase. Ol, olivine. Data source as in Fig. 1.  
685

686 Fig. 3. Relationships between Mg/(Mg + Fe<sup>2+</sup>) and Cr/(Cr + Al) atomic ratios of  
687 chromian spinels in plutonic rocks. Upper and lower panels are for dunites and other  
688 possible cumulates, and for peridotites, respectively. (a) Mid-ocean ridges. (b) Arcs.  
689 (c) Oceanic hotspots. Peridotites, lherzolites and harzburgites. Pl, plagioclase. Ol,  
690 olivine. Data source as in Fig. 1.

691  
692 Fig. 4. Relationships between TiO<sub>2</sub> contents and Fe<sup>3+</sup>/(Cr + Al + Fe<sup>3+</sup>) atomic ratios  
693 of chromian spinels in plutonic rocks. Upper and lower panels are for dunites and  
694 other possible cumulates, and for peridotites, respectively. (a) Mid-ocean ridges. (b)  
695 Arcs. (c) Oceanic hotspots. Peridotites, lherzolites and harzburgites. Pl, plagioclase.  
696 Ol, olivine. The fields for MOR (a) and hotspot (c) plutonics are shown in the panel  
697 (b). The field for MORB spinels (Arai, 1992) is shown in the panel (a) for

698 comparison. Data source as in Fig. 1. Fields for the main clusters of mid-ocean ridge  
699 (MOR) and hotspot spinels are shown in the panel (b).

700

701 Fig. 5. Photographs of discordant dunites. (a) Outcrop of discordant dunites (D)  
702 within foliated mantle harzburgite from Wadi Rajmi, the northern Oman ophiolite.  
703 (b) Photomicrograph of a partially serpentinized discordant dunite from Wadi Rajmi.  
704 Plane-polarized light. (c) Outcrop of a discordant dunite (D; selectively eroded)  
705 from the Lizard ophiolite. (d) Photomicrograph of a chromian spinel grain with  
706 high-Ti exsolution blebs (brighter) in a partially serpentinized discordant dunite  
707 from the Lizard ophiolite. Reflected plane-polarized light. Note the bright band  
708 fringing the right-side margin is remnants of carbon coating.

709

710 Fig. 6. Chromian spinel compositions in discordant dunites from the Oman and  
711 Lizard ophiolites. Note the different compositional characteristics between the two  
712 dunite spinels. (a)  $\text{TiO}_2$  vs.  $\text{Cr}/(\text{Cr} + \text{Al})$  atomic ratio. Compare with Figure 1. (b)  
713  $\text{TiO}_2$  vs.  $\text{Fe}^{3+}/(\text{Cr} + \text{Al} + \text{Fe}^{3+})$  atomic ratios. Compare with Figure 4. (c) Cr-Al-  $\text{Fe}^{3+}$   
714 atomic ratios. The fields for MOR and hotspot dunites (Figure 2) are shown in the

715 panel (b).

716

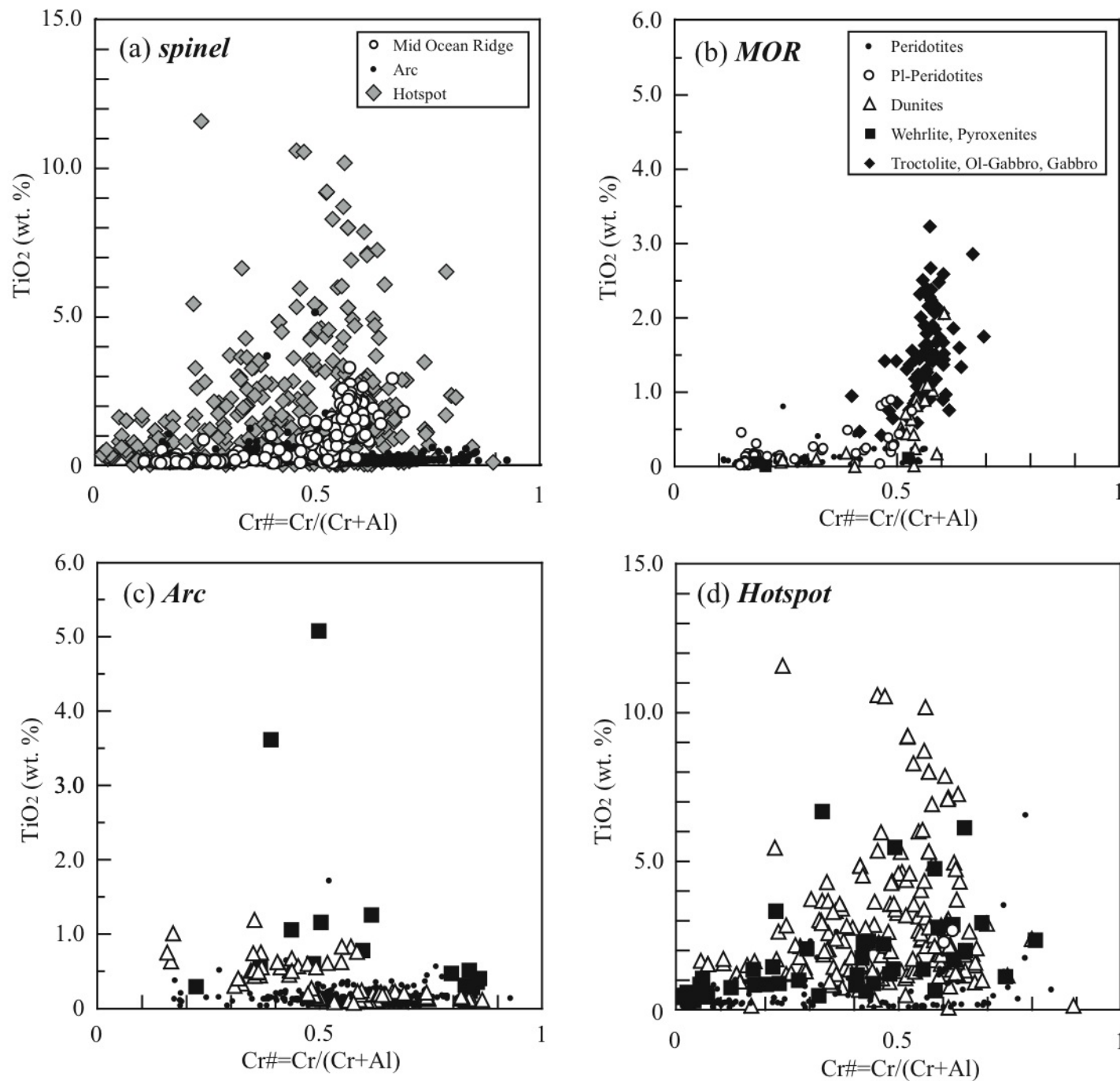


Fig.1 Arai et al.

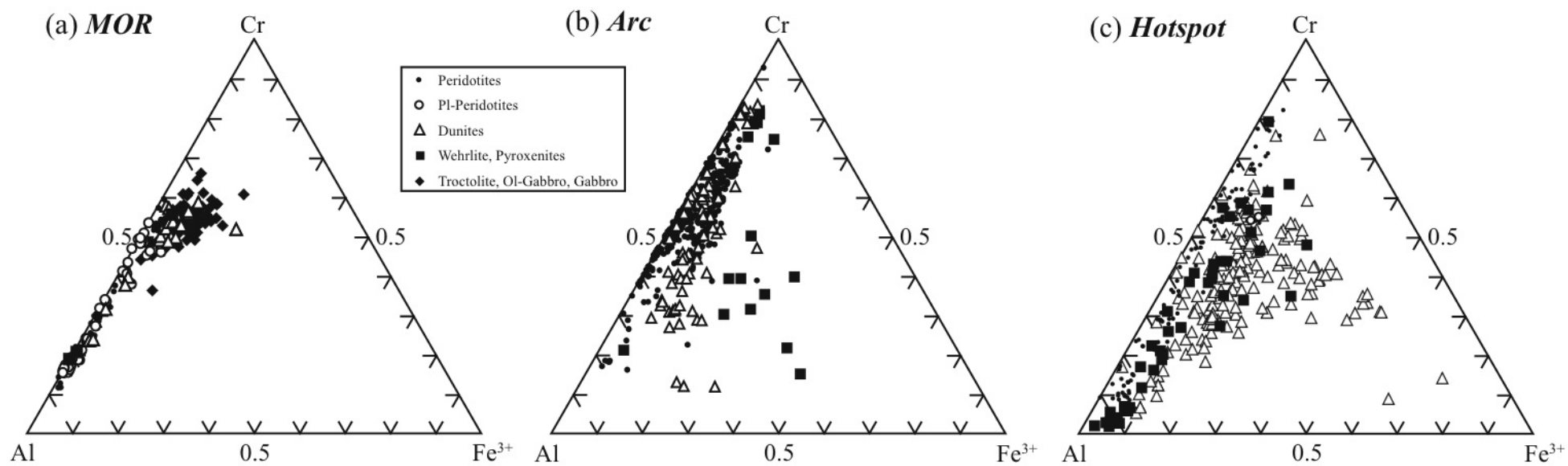


Fig. 2 Arai et al.

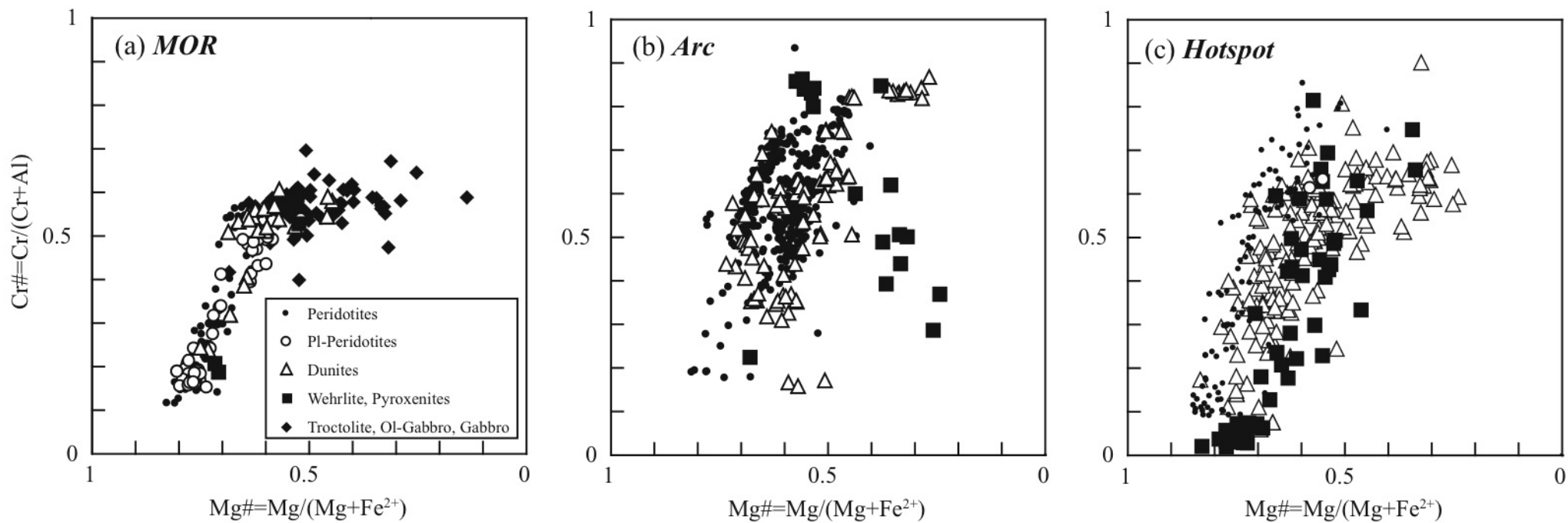


Fig. 3 Arai et al.

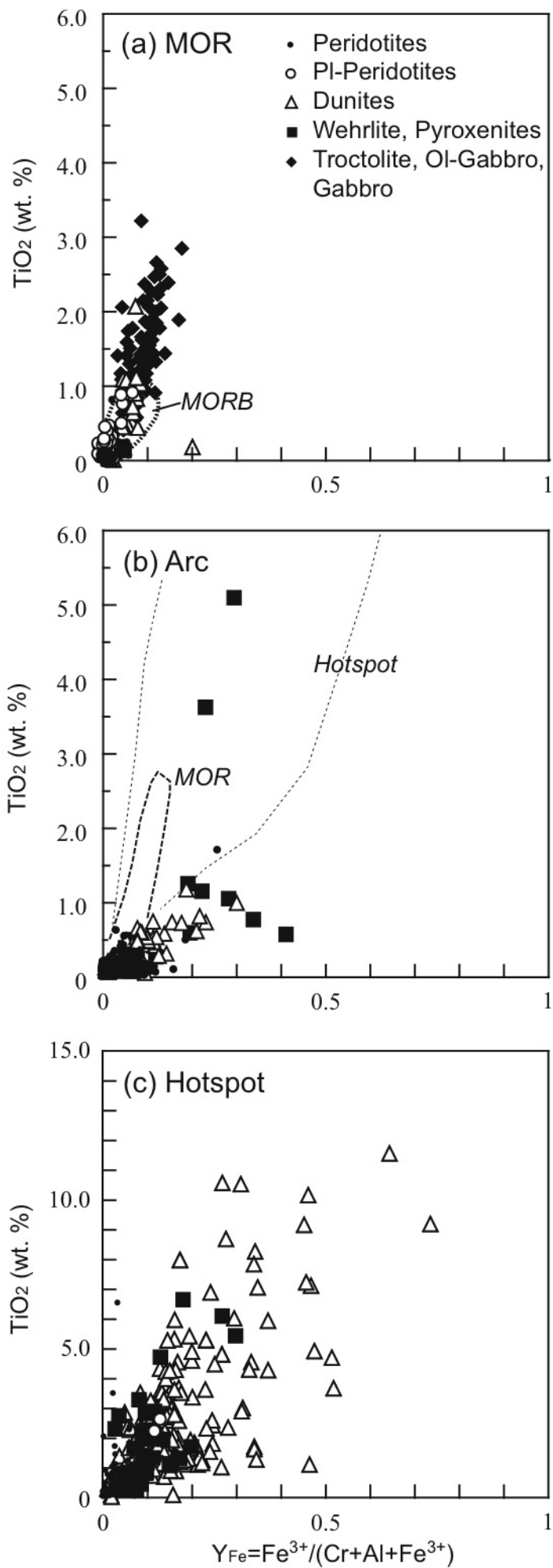


Fig. 4 Arai et al.



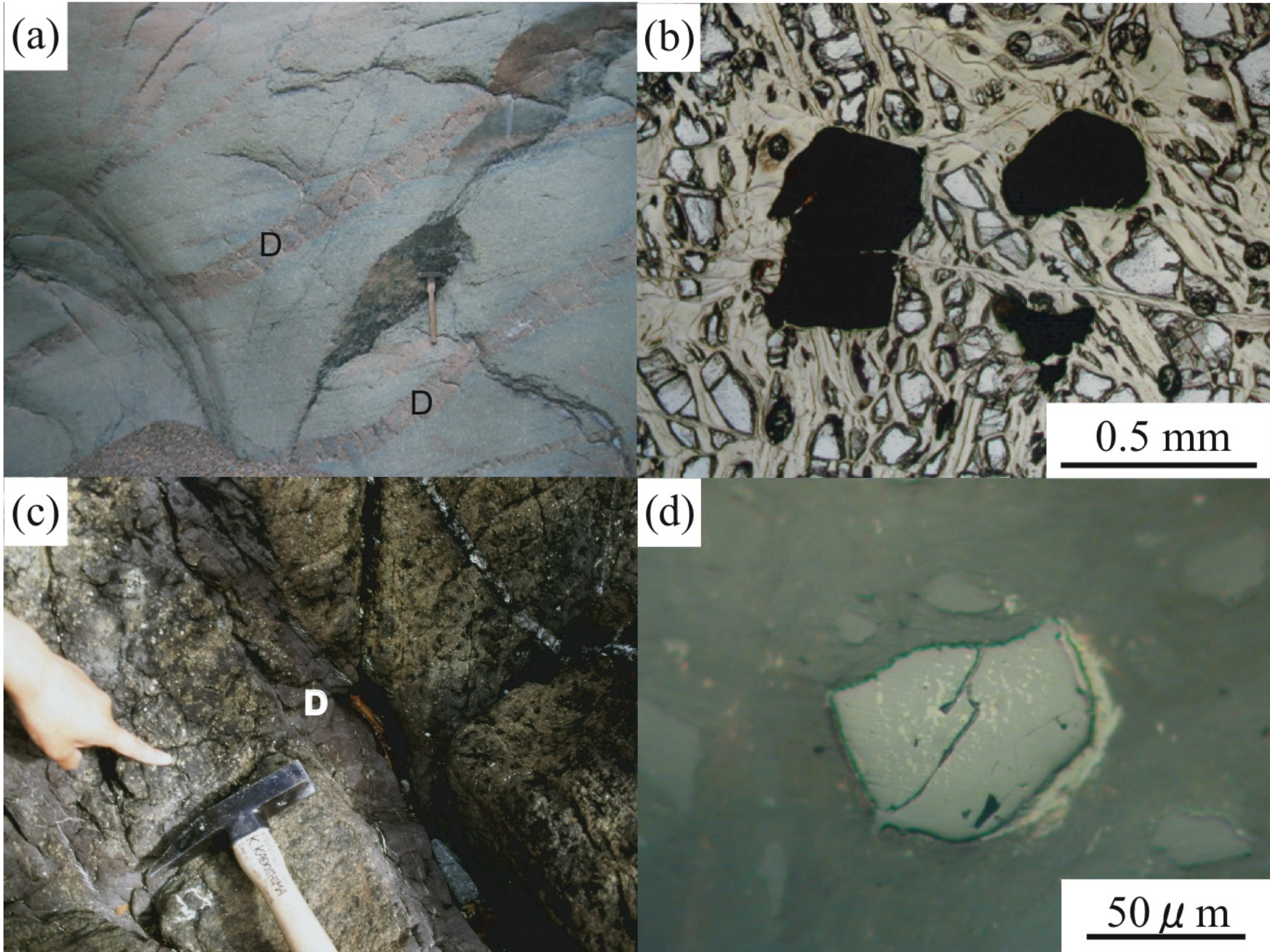


Fig. 5 Arai et al.

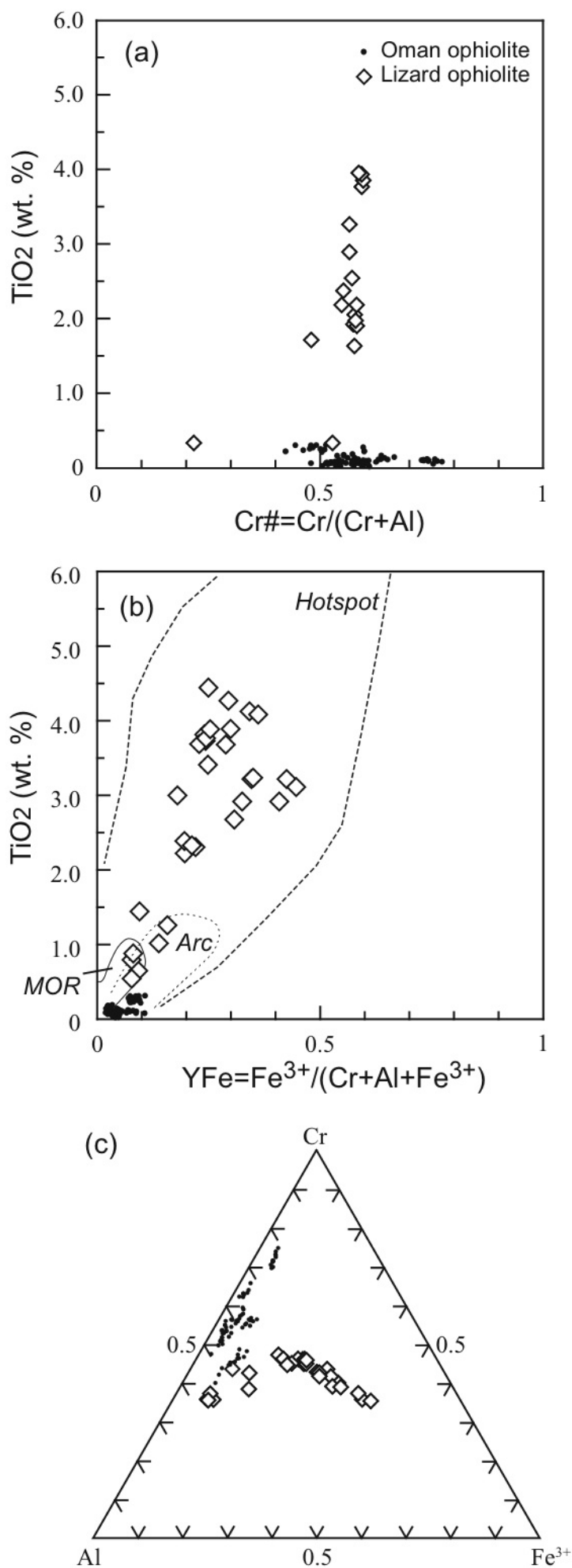


Fig. 6 Arai et al.